Available online at www.sciencedirect.com
SCIENCE DIRECT
Free Radical Biology & Medicine 41 (2006) 165–174
www.elsevier.com/locate/freeradbiomed

Original Contribution

Adriamycin promotes macrophage dysfunction in mice

Reto Asmis [a,*], Mu Qiao [a], Randall R. Rossi [b], Jill Cholewa [c], Li Xu [c], Lars M. Asmis [d]

[a] *Division of Nephrology, University of Texas Health Science Center at San Antonio and South Texas Veterans Health Care System, 7703 Floyd Curl Drive, MSC 7882, San Antonio, TX 78229, USA*
[b] *University of Rochester Medical Center, Rochester, NY, USA*
[c] *Graduate Center for Nutritional Sciences, University of Kentucky, Lexington, KY, USA*
[d] *Division of Hematology, University Hospital, Zürich, Switzerland*

Received 1 July 2005; revised 10 March 2006; accepted 31 March 2006
Available online 18 April 2006

Abstract

Impaired wound healing contributes to the morbidity and mortality associated with adriamycin chemotherapy. Macrophages are essential for tissue repair and loss of macrophage function leads to impaired wound healing. We recently showed that adriamycin is a potent inducer of thiol oxidation and cell injury in cultured macrophages (FASEB J. 19:1866–1868; 2005). Here we tested the hypothesis that adriamycin also promotes oxidative stress and macrophage dysfunction in vivo. We treated FVB mice twice a week either with low doses of adriamycin (4 mg/kg) or with the same volume of saline by tail vein injection for a total of 8 injections. Wound healing was significantly delayed in adriamycin-treated mice. The number of resident peritoneal macrophages was decreased by 30% and macrophage recruitment in response to thiogycolate stimulation was decreased by 46% in mice treated with adriamycin. LPS-induced TNFα and IL-1β secretion from macrophages of adriamycin-treated mice was decreased by 28.7 and 29.5%, respectively, compared to macrophages isolated from saline-injected mice. Peritoneal macrophages isolated from adriamycin-treated mice also showed increased formation of reactive oxygen species and enhanced protein-S-glutathionylation. In summary, our results show that low cumulative doses of adriamycin are sufficient both to promote sustained thiol oxidative stress and macrophage dysfunction in vivo and to delay tissue repair, suggesting that macrophage dysfunction contributes to impaired wound healing associated with adriamycin chemotherapy.

Keywords: Adriamycin; Macrophage; Thiol oxidation; Cell death; Wound healing; Protein-*S*-glutathionylation

Introduction

Adriamycin (doxorubicin) is a potent antibiotic widely used in the chemotherapy of solid and hematopoietic tumors [1]. In addition to its chronic and irreversible cardiotoxicity, adriamycin also has well-known acute and reversible side effects such as nausea, vomiting, myelosuppression, and arrhythmia. Subacute side effects such as immunological deficits and impaired wound healing have also been described, suggesting that adriamycin may also promote sustained damage in noncardiac cells and tissues [2–5]. In cancer patients being treated aggressively with chemotherapy, impaired musculofascial and enteric healing are a major cause of morbidity and mortality [6], but the mechanisms underlying impaired wound healing in these patients are only poorly understood. Macrophages play a key role in tissue repair and wound healing [7]. Through the release of chemoattractants, growth factors, protease, and extracellular matrix molecules, macrophages orchestrate the complex processes of cell proliferation and functional tissue regeneration. Adriamycin-induced macrophage dysfunction may therefore contribute to impaired

Abbreviations: DCFH, 6-carboxy-2′,7′-dichlorodihydrofluorescein diacetate di(acethoxymethyl) ester; DTT, dithiothreitol; EMSA, electrophoretic mobility-shift assay; FBS, fetal bovine serum; GSH, reduced glutathione; GSSG, glutathione disulfide (oxidized glutathione); IL, interleukin; INF, interferon; HPLC, high-performance liquid chromatography; KP_i, potassium phosphate buffer; NaP_i, sodium phosphate buffer; PBS, phosphate-buffered saline; PMSF, phenylmethylsulfonyl fluoride; PSSG, protein-conjugated glutathione; ROS, reactive oxygen species; TNF, tumor necrosis factor; WBC, white blood cell.

* Corresponding author. Fax: +1 210 567 0517.
E-mail address: asmis@uthscsa.edu (R. Asmis).

0891-5849/$ - see front matter © 2006 Elsevier Inc. All rights reserved.
doi:10.1016/j.freeradbiomed.2006.03.027

wound healing. The effect of adriamycin therapy on macrophages in vivo has not been studied in detail.

The antitumoricidal activity of anthracyclines is mainly due to the irreversible damage to tumor cell DNA [8]. Adriamycin is also a potent inducer of intracellular oxidative stress because of its ability to generate highly reactive oxygen-derived radicals [1,8,9]. In cardiomyocytes, adriamycin-induced reactive oxygen species (ROS) formation is believed to occur at the inner mitochondrial membrane. Adriamycin binds with high affinity to cardiolipin, a phospholipid and major component of mitochondrial membranes required for full activity of the respiratory chain enzymes, cytochrome *c* oxidase and NADH dehydrogenase as well as cytochrome *c* reductase [10,11]. Once binding occurs, adriamycin can act as an alternate electron acceptor in the respiratory chain. This results in the reduction of adriamycin to its semiquinone free radical form. Adriamycin can also redox-cycle with nonmitochondrial flavoenzymes such as NADPH-cytochrome P450 reductase, NADH-cytochrome *b* reductase, and nitric oxide synthases [12,13]. It is not clear which enzymes are responsible for adriamycin reduction in intact cells. However, once in its reduced form, adriamycin spontaneously autooxidizes in the presence of oxygen, generating superoxide and subsequently other ROS, which can promote lipid peroxidation [14].

While cardiomyocytes are particularly sensitive to adriamycin toxicity due to their dependence on mitochondria for ATP synthesis, adriamycin is likely to also promote oxidative stress in other tissues. We recently demonstrated that in cultured human macrophages adriamycin promotes the formation of glutathione disulfide and increases protein-*S*-glutathionylation prior to cell injury [15]. Treatment of cells with scavengers of superoxide and peroxyl radicals blocked adriamycin-induced ROS formation, but did not prevent macrophage injury, suggesting that in macrophages thiol oxidation, rather than one-electron redox cycling and ROS generation, mediates adriamycin-induced cell damage.

In the present study we investigated whether treatment of mice with low doses of adriamycin that are sufficient to impair wound healing also promotes thiol oxidative stress in macrophages and alters macrophage responsiveness to cell stimulation.

Materials and methods

Animals

FVB mice were obtained from Jackson Laboratories (Bar Harbor, ME) and were maintained under controlled animal room conditions. The animals were fed a laboratory diet and water ad libitum. All animal procedures were approved by the University of Kentucky Institutional Animal Care and Use Committee, which is certified by the American Association of Accreditation of Laboratory Animal Care.

Drug treatment

Female 8-week-old FVB mice (mean body weight = 22.5 ± 0.3 g) were randomly distributed into two groups. Adriamycin (Bedford Laboratories, Bedford, OH) was diluted in saline to a final concentration of 0.4 mg/ml and injected iv at 4 mg/kg twice a week (Monday and Thursday) for a total of 8 injections (on Days 1, 3, 7, and 10 and Days 28, 31, 35, and 38) (Fig. 1). Control animals were injected with the same volume of saline. Animals were not treated for 2 weeks between the first four and the last four injections to allow for the recovery of the blood cell count. The mean cumulative dose of adriamycin administered was 93 mg/m^2. This treatment protocol was adapted from a protocol that was developed and standardized based on the clinical application of adriamycin and the clinically relevant chronic cardiotoxicity induced by this treatment in FVB mice [16,17]. After the last adriamycin injection, mice were allowed to recover for 10 days prior to wounding or harvesting tissues. At this point, we observed no significant difference in the body weight between both groups of animals. Mean body weights were 24.4 ± 0.7 and 23.8 ± 0.4 g for saline and adriamycin treatment groups, respectively.

Experimental procedures

Blood was drawn biweekly under isoflurane anesthesia from the retro-orbital plexus of all animals and platelet, red blood cell, lymphocyte, and monocyte counts were monitored with a Baker B9118 + CP blood analyzer. Ten days after the last

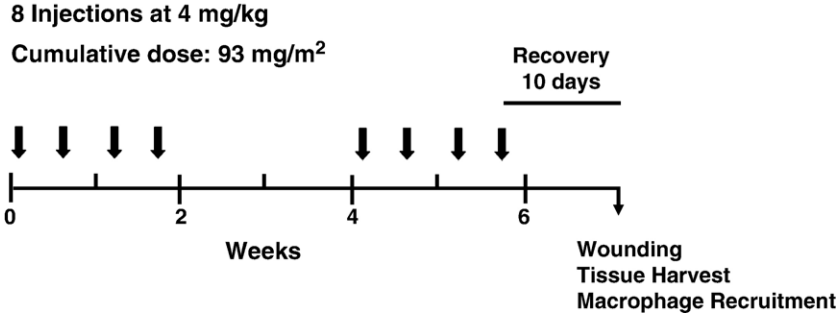

Fig. 1. Schematic outline of the experimental design. Female FVB mice were injected iv with either saline or adriamycin (4 mg/kg) twice a week (Monday and Thursday) for a total of 8 injections. Animals were not treated for 2 weeks between the first four and the last four injections to allow for the recovery of the blood cell count. The mean cumulative dose of adriamycin administered was 93 mg/m^2. After the last injection and a 10-day recovery period, either mice were wounded and wound healing was assessed or mice were euthanized and tissues and peritoneal macrophages were harvested.

injections, animals were either euthanized by CO_2 inhalation and cervical luxation for macrophage harvest and tissue collection or anesthetized by intraperitoneal injection of ketamine (95 μg/g body weight) plus xylazine (5 μg/g body weight) and subjected to wounding. Resident peritoneal cells were harvested by lavage with 5 ml of ice-cold Dulbecco's modified Eagle medium supplemented with 2 mM L-alanyl-L-glutamine (GLUTAMAX-1, GIBCO BRL, Carlsbad, CA), 1% v/v nonessential amino acids (GIBCO BRL), penicillin G/streptomycin (100 U/l and 100 μg/ml, respectively, GIBCO BRL), referred to from here on simply as culture medium. Cell viability was determined by trypan blue extrusion and was >95% in all cell preparations. Immediately after peritoneal lavage, heart and spleen were removed from each animal and weighed.

Wound healing

Wounding was performed according to a procedure described by Mori et al. [18]. Briefly, mice were shaved and cleaned with Betadine and 70% ethanol, and excisional full-thickness skin wounds were generated aseptically on the dorsal skin by picking up a fold skin at the midline and punching through two layers of skin with a sterile disposable biopsy punch with a diameter of 4 mm. This generated two wounds simultaneously, one wound on each side of the midline. The same procedure was repeated twice on the same animal, generating a total of four wounds, each with a diameter of 4 mm. After 0, 1, 3, 6, 8, and 11 days, each wound was photographed with a MicroFire digital camera (Olympus, Melville, NY) and wound areas were quantified with ImagePro Software.

Macrophage recruitment

Saline (n = 8) and adriamycin-treated mice (n = 8) were injected ip with 3 ml 4% (w/v) thioglycolate solution. Three days after thioglycolate injections, peritoneal cells were harvested by lavage with 4 ml of culture medium as described above. Cells were counted and plated at a density of 1.5×10^5/ml in culture medium supplemented with 10% FBS and cultured in a humidified atmosphere at 5% CO_2. After 4 h, nonadherent cells were removed through washing with culture medium and adherent cells were lysed in 0.5 N NaOH solution. Protein levels were measured determined with bicinchoninic acid (Pierce, Rockford, IL) using bovine serum albumin as a standard.

TNFα, IL-1β, VEGF, and TGF-β assays

Peritoneal cells were plated at a density of 2×10^5/ml in culture medium supplemented with 10% FBS and cultured in a humidified atmosphere at 5% CO_2. After 4 h, nonadherent cells were removed through washing with culture medium and adherent cells were incubated for 48 h either in the absence or in the presence of LPS (1 μg/ml) plus interferon (INF)-γ (100 U/ml). Cell protein was determined in each well by the Lowry method (Bio-Rad Laboratories, Hercules, CA) and standardized with bovine serum albumin. TNFα, IL-1β, VEGF, and TGF-β concentrations in cell supernatants were measured with commercial enzyme-linked immunosorbant assays (ELISA) kits purchased from R and D Systems (TNFα, IL-1β, VEGF) and Biosource International (TGF-β, Camarillo, CA).

Formation of intracellular reactive oxygen species

Formation of intracellular ROS was assessed with the redox-sensitive dye 6-carboxy-2′,7′-dichlorodihydrofluorescein diacetate di(acethoxymethyl) ester (DCFH, Molecular Probes). Peritoneal cells were plated at 0.3×10^6 cells/ml for 3 h and nonadherent cells were removed by washing. Macrophages were loaded for 1 h at 37°C with 10 μg/ml DCFH, washed, and then incubated for 9 h at 37°C. Fluorescence was monitored in a Fusion plate reader (Packard) set at an excitation wavelength of 485 ± 10 nm and emission wavelengths of 535 ± 12.5 nm. Rates of dye oxidation were normalized to cell protein.

Determination of cellular glutathione

Macrophages were washed with PBS and harvested by scraping. Each sample was split into three 200-μl aliquots, one for the determination of DNA as a measure of cell number, and one each for the determination of glutathione disulfide (GSSG) and total glutathione (GSH + GSSG). Samples were prepared as described previously [15]. Briefly, the samples designated for GSSG determination were supplemented with *N*-ethylmaleimide (7.4 mM) to alkylate free thiol groups. Proteins were precipitated with 100 μl cold 18% perchloric acid and supernatants were neutralized with 1 M KP_i (pH 7.0). Samples were diluted with 0.1 M KP_i (pH 7.0) and reduced with 10 mM dithiothreitol for 60 min at room temperature. Glutathione was derivatized in the presence of 11 mM *o*-phthalaldehyde and separated by reverse-phase HPLC. HPLC analysis was performed on a Jasco HPLC system equipped with a spectrofluorometer (FP-920, Jasco Inc.) set to an excitation wavelength of 340 nm and an emission wavelength of 420 nm. Glutathione was separated isocratically on a Brownlee 3-cm C18 ODS guard column (5 μm) and a Brownlee 22-cm C18 ODS analytical column (5 μm) with 21 mM propionate buffer (in 35 mM NaP_i, pH 6.5)/acetonitrile (95/5 by vol) at a flow rate of 1.2 ml/min. Levels of reduced glutathione (GSH) were calculated as the difference between GSH + GSSG and GSSG.

Determination of protein-bound glutathione

Macrophages were washed with PBS and harvested by scraping; each sample was split into two aliquots, one for the determination of DNA (200 μl) and one for the determination of protein-bound glutathione (500 μl). Proteins were precipitated as described above. Protein pellets were resuspended in 0.5 M NaOH and neutralized with 1 M KP_i (pH 7.0). Glutathione was released by reduction with 7 mM dithiothreitol for 1 h at room temperature. Proteins were precipitated, and the supernatants were analyzed for glutathione, as described above.

Measurement of cellular DNA

The quantity of DNA was determined fluorometrically using the PicoGreen DNA Quantitation Kit (Molecular Probes, Eugene OR) as described previously [15]. Fluorescence was measured in a Fusion plate reader (Packard) set to an excitation wavelength of 485 nm and an emission wavelength of 535 nm.

Electrophoretic mobility-shift assay (EMSA)

Nuclear extracts were prepared using the Nuclear Extract kit (Active Motif, Carlsbad, CA). To generate the DNA probe containing the κB binding sequence, the double-stranded oligonucleotide sequence of 5-AGTTGAGGGGACTTTCC-CAGGC-3, 3-TCAACTC-CCCTGAAAGGGTCCG-5 (Promega, Madison, WI), was end-labeled with [γ-^{32}P]ATP using T4 polynucleotide kinase (New England Biolabs, Ipswich, MA) [19]. DNA binding reactions were performed by adding 1 μg nuclear protein to 4 μl binding buffer containing 50 mM Hepes (pH 7.9), 250 mM KCl, 1 mM EDTA, 12.5 mM DTT, 50% glycerol, 0.25% Nonidet P-40, and 0.4 μg poly(dI-dC). After 10 min on ice, the labeled oligonucleotide was added (2 μl, 0.1 pmol, 7×10^4 cpm) and the mixture was incubated for 20 min at room temperature. Samples were subjected to 6% polyacrylamide gel electrophoresis at 150 V in TBE buffer (45 mM Tris base, 45 mM boric acid, 0.25 mM EDTA) for 3–4 h.

Nuclear extract from HeLa cells was prepared according to the method of Dignam et al. [20] and 5 μg extract in 20 mM Hepes, pH 7.9, 20% v/v glycerol, 0.1 M KCI, 0.2 mM EDTA, 0.5 mM PMSF, and 0.5 mM DTT was loaded as a positive control. The gel was then dried under vacuum and bands were visualized and quantified using a PhosphorImager (FLA-500, Fugifilm Medical Systems USA, Stamford, CT). The intensities of the bands from the samples were normalized to the band intensity of the positive control, which was arbitrarily set at 1.0.

Statistical analysis

Results are presented as means ± SE. Data were compared among groups using an unpaired *t* test for two groups or ANOVA for multiple groups. Multiple-group comparisons were performed using the Student-Newman-Keuls method. Results were considered significant at the $P < 0.05$ level. Statistical analysis was performed utilizing SigmaStat (SPSS).

Results

Impaired wound healing in response to low doses of adriamycin

Impaired wound healing after adriamycin administration at single doses is well documented [4,5,21], but the effect on wound healing of clinically more relevant regimens, i.e., multiple injections of low doses, has not been reported. We therefore investigated whether repeated injections of adriamycin at low doses (4 mg/kg) also result in impaired wound healing To minimize any indirect effects of cardiotoxicity, we chose a cumulative dose (27.8 mg/kg, 93 mg/m^2) 25% below the mean cumulative cardiotoxic dose for adriamycin in FVB mice (36.4 mg/kg, 121.5 mg/m^2) [16] and well below the recommended maximal cumulative dose in humans (500–600 mg/m^2) [22]. High doses of adriamycin (40 mg/kg) have been reported to increase the heart to body weight ratio in FVB mice by 51% [23]. We found that the hearts in mice treated with low doses of adriamycin showed only a 12% increase in the heart weight/body weight ratios ($P = 0.017$), indicating that this low cumulative dose of adriamycin induced only minor cardiac hypertrophy. Mean heart weight/body weight ratios were 6.5 ± 0.3 mg/g in adriamycin-treated mice compared to 5.8 ± 0.3 mg/g in control mice. We found no significant difference in the body weight between both groups of animals. To further reduce the impact of any residual acute toxicity of the drug, animals were allowed to recover for 10 days after the last injection (Fig. 1).

To determine whether repeated injections of adriamycin at low doses also result in impaired wound healing, we generated four 4 mm full-thickness excisional skin wounds on the back of six saline- and six adriamycin-treated FVB mice and monitored wound closure for 11 days. Initially, we observed no difference in wound healing between both groups (Fig. 2). One day after wounding, mean wound size was reduced by 24% in saline-treated mice and 22% in adriamycin-treated mice. However, after 3 days, we observed a significant delay in wound closure in adriamycin-treated mice. Wound closure in saline-treated mice was 65% complete compared to only 48% in adriamycin-treated mice. Adriamycin-treated animals required approximately 6 days to achieve 65% wound closure, i.e., 3 days longer than saline-treated mice. A similar delay was estimated for 80% wound closure, approximately 7 days for saline-treated mice versus 10 days for adriamycin-treated mice.

Effects of low doses of adriamycin on blood cell counts

Both immunosuppressive effects and immunoaugmentation have been observed in response to adriamycin [3]. In patients, high doses of adriamycin induce reversible myelosuppression [24]; however, the effects of low doses of adriamycin on white blood cell (WBC) counts have not been reported. We therefore investigated whether myelosuppression may have contributed to the reduction in peritoneal macrophages we observed in FVB mice after low-dose adriamycin treatment. Blood cell counts were monitored in all mice twice weekly throughout the study. We observed no significant change in blood monocyte counts during both treatment periods in which mice received adriamycin (Fig. 3). However, 4 days after the first and 7 days after the second treatment period, we observed a dramatic increase in blood monocytes. After the first series of injection, blood monocyte counts increased 6.5-fold compared to saline-treated mice, but monocyte counts returned to control levels 11 days after the fourth adriamycin injection. After the second injection series, the increase in monocytes was less pronounced, 3.8-fold compared to saline control, and monocyte counts returned to control levels after the 10-day recovery period. We obtained very similar results for

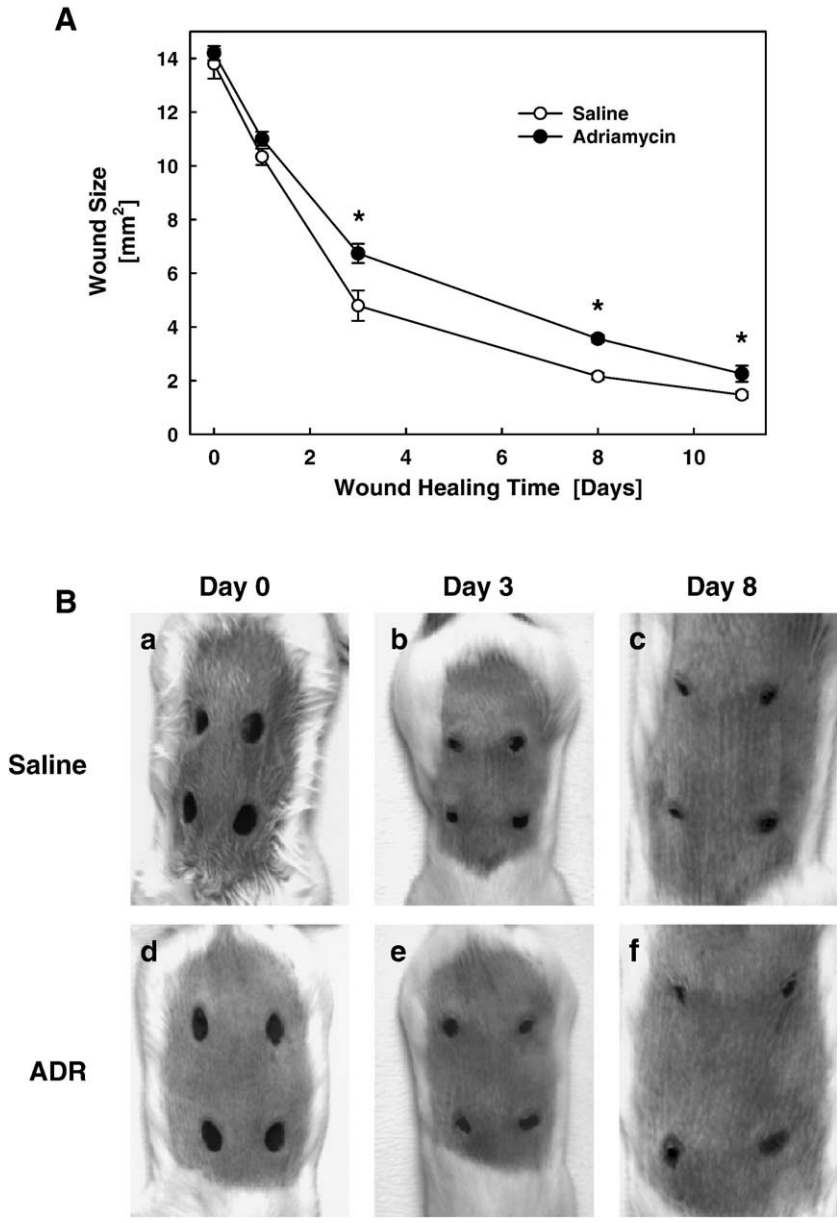

Fig. 2. Impaired wound healing in mice treated with low doses of adriamycin. (A) Ten days after the last injection, saline- ($n = 6$) and adriamycin-treated ($n = 6$) mice received four 4 mm excisional full-thickness skin wound on the dorsal skin. After 0, 1, 3, 6, 8, and 11 days, each wound was photographed with a digital camera and wound areas were quantified with ImagePro Software. Initial wound areas (Day 0) were 13.8 ± 0.6 and 14.2 ± 0.3 mm^2 in saline- and adriamycin-treated mice, respectively. On Days 3–11 wound healing was significantly delayed in adriamycin-treated mice compared to control animals (*$P < 0.05$). (B) Photographs of typical wounds on mice after treatment with saline (a–c) and adriamycin (ADR) (d–f).

lymphocytes. In contrast to high doses of adriamycin, low-dose adriamycin treatment appears to promote delayed but completely reversible leukocytosis.

After completing the treatment protocol, including the 10-day recovery period, blood cell and platelet counts in both the saline and the adriamycin treatment groups were not statistically different between adriamycin- and saline-treated mice (Table 1), indicating that adriamycin-treated mice had fully recovered from any acute effects of the drug. Compared to their initial values at the beginning of the study (Day 1) WBC counts were decreased by 25% in saline-treated mice and 26% in adriamycin-treated mice. This decrease appears to be age related. Differential analysis of the WBC fraction revealed no statistically significant difference in the lymphocyte, monocyte, and granulocyte counts between the two groups.

Impaired macrophage recruitment after low-dose adriamycin treatment

Macrophage recruitment is essential for normal tissue repair and wound healing [7]. To determine whether low-dose adriamycin treatment alters macrophage recruitment in mice, we first performed peritoneal lavages in saline and adriamycin-treated mice to measure their resident peritoneal macrophage

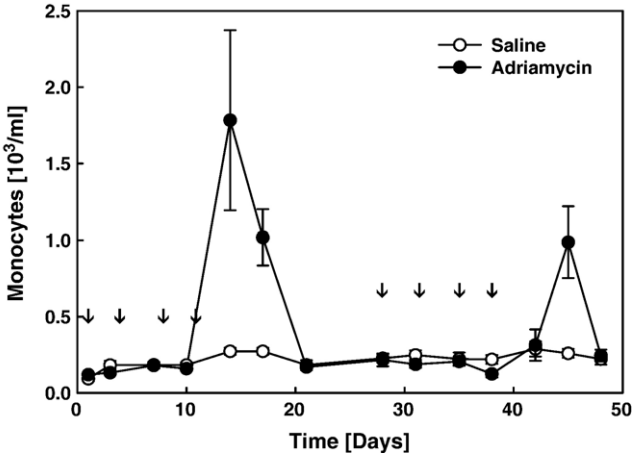

Fig. 3. Effect of low-dose adriamycin treatment on blood monocyte levels in FVB mice. Saline (○) or adriamycin (●) was injected on the days indicated (↓) and blood monocyte counts were monitored biweekly as described under Materials and methods.

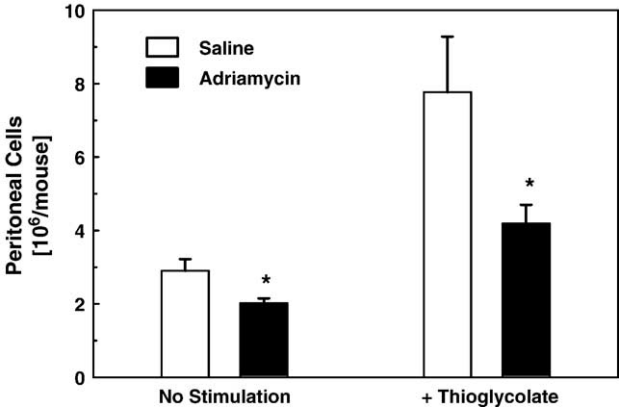

Fig. 4. Impaired macrophage recruitment after low dose adriamycin treatment. FVB mice were treated with either saline (□, $n = 13$) or low doses of adriamycin (■, $n = 15$) and macrophages were isolated as described under Materials and methods. A second group of saline- ($n = 8$) and adriamycin-treated ($n = 8$) mice were injected with thioglycolate 3 days prior to performing peritoneal lavages to stimulate macrophage recruitment. Results are shown as mean ± SE. * $P < 0.05$ versus saline treatment.

content. Cell counts revealed that the mean cell yield was 30% lower in adriamycin-treated mice ($P < 0.05$) compared to saline-treated control animals (Fig. 4, No Stimulation). Cell viability was not decreased in the cell preparations from adriamycin-treated mice, indicating that enhanced cell death is not a likely explanation for the hypocellularity induced by adriamycin. After plating an equal number of peritoneal cells from each mouse and removing nonadherent cells by gentle washing, we lysed the cells and measured the protein content in each well to determine if the macrophage content of the peritoneal cell suspension was different between saline- and adriamycin-treated mice. No difference in the protein values was observed, indicating that the lower yield of peritoneal cells obtained from adriamycin-treated mice reflected a lower content in resident peritoneal macrophages.

To stimulate macrophage recruitment, a second group of eight saline and eight adriamycin-treated mice was injected intraperitonealy with thioglycolate solution to induce peritonitis. Thioglycolate increased the number of peritoneal cells in saline-treated mice 2.7-fold, from $2.9 \pm 3.2 \times 10^6$ to $7.8 \pm 1.5 \times 10^6$, but only 2-fold, from $2.1 \pm 0.1 \times 10^6$ to $4.2 \pm 0.5 \times 10^6$ in adriamycin-treated mice (Fig. 4, + Thioglycolate). Total macrophage content after thioglycolate treatment was 46% lower in adriamycin-treated mice ($P < 0.05$) compared to saline-treated control animals, indicating that macrophage recruitment is severely impaired after adriamycin treatment.

Table 1
Blood cell counts in adriamycin-treated and saline-treated control mice

	Day 1	After recovery period	
		Saline	Adriamycin
RBC (10^6/ml)	9.9 ± 0.2	10.0 ± 0.2	11.0 ± 0.9
Platelets (10^6/ml)	1.8 ± 0.1	2.0 ± 0.1	2.0 ± 0.2
WBC (10^6/ml)	10.8 ± 0.6	8.1 ± 0.5*	8.0 ± 1.3**

Blood cell counts were determined in FVB mice injected with either saline ($n = 13$) or adriamycin ($n = 15$) as described under Materials and methods. Blood samples were analyzed on the Baker B9118 + CP blood analyzer. Results from the first day of the treatment protocol (Day 1) and after the 10-day recovery period (Fig. 1) are shown as mean ± SE. * $P = 0.001$ and ** $P = 0.003$ versus Day 1.

Impaired macrophage function after low-dose adriamycin treatment

Next we examined whether other macrophage responses were also impaired after low-dose adriamycin treatment in mice. To this end we isolated peritoneal macrophages from saline- and adriamycin-treated mice and stimulated the cells for 48 h with LPS (1 μg/ml) plus IFNγ (100 U/ml). Macrophage function was assessed as the ability of cells to produce and secrete IL-1β, TNFα, VEGF, and TGF-β into the cell supernatant in response to cell stimulation. We found that secretion of IL-1β and TNFα was reduced by 30 and 29%, respectively, in macrophages from adriamycin-treated mice compared to macrophages isolated from control mice (Fig. 5). VEGF secretion was also reduced by 20%, but the difference did not reach statistical significance ($P = 0.08$). In contrast, release of TGF-β was not significantly altered by adriamycin treatment (Fig. 5). We also observed no difference in basal TGF-β release from macrophages isolated from saline- and adriamycin-treated mice (not shown).

LPS-induced NF-κB activation is not impaired in macrophages from adriamycin-treated mice

In macrophages, LPS-induced IL-1β, TNFα, and VEGF formation is regulated by NF-κB [25]. Multiple steps along the NF-κB activation signaling pathway are sensitive to inactivation by oxidative stress and thiol oxidation [26–30]. We therefore examined whether LPS-induced activation of NF-κB was impaired in macrophages from adriamycin-treated mice. Peritoneal macrophages (2×10^6/mouse) isolated from nine adriamycin-treated and nine control mice were stimulated for 2 h with LPS (1 μg/ml) plus IFNγ (100 U/ml). To obtain sufficient nuclear material to perform EMSA on macrophages

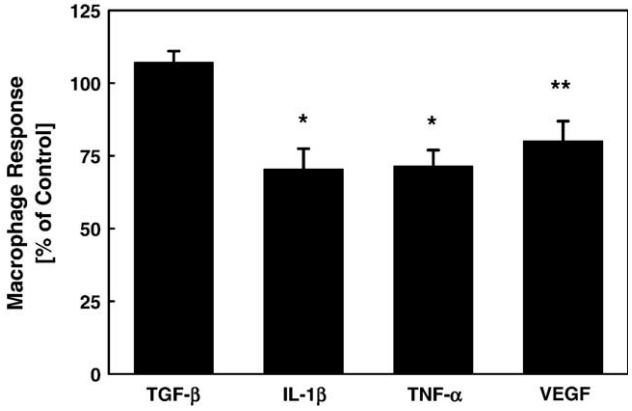

Fig. 5. Impaired cytokine and growth factor release in macrophages isolated from adriamycin-treated mice. Peritoneal macrophages were isolated from saline- (n = 13) and adriamycin-treated (n = 15) mice 12 days after the last injection (day 50) and plated at 2 × 10^5/ml as described under Materials and methods. Macrophages were incubated for 48 h either in the absence or presence of LPS (1 μg/ml) plus interferon (INF)-γ (100 U/ml). TNFα, IL-1β, VEGF, and TGF-β concentrations in the cell supernatants were measured using ELISA. All values shown are for macrophages from adriamycin-treated mice and are presented as a percentage of control (macrophages from saline-treated mice). TGF-β (100% = 906 ± 53 pg/mg), IL-1β (100% = 546 ± 58 pg/mg), TNFα (100% = 4.70 ± 0.28 ng/mg), VEGF (100% = 80 ± 6 pg/mg). Results are shown as mean ± SE. * $P < 0.05$, ** $P = 0.08$.

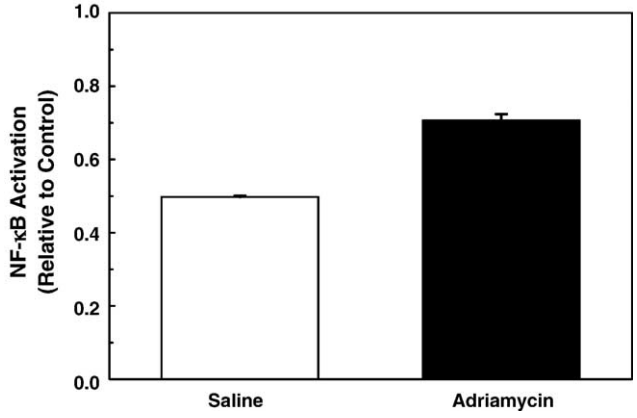

Fig. 6. No reduction in LPS-Induced NF-κB activation in macrophages isolated from adriamycin-treated mice. Peritoneal macrophages were isolated from saline- (n = 9) and adriamycin-treated (n = 9) mice 12 days after the last injection (Day 50) and plated at 2 × 10^6/ml. Nuclear extracts were prepared from each well and pooled for each group. EMSA were performed as described under Materials and methods. The two pooled samples were analyzed twice in independent assays for NF-κB activity. Nuclear extract from HeLa cells (5 μg) was loaded as positive controls. Band intensities obtained for the samples were normalized to the band intensity obtained for the positive control, which was arbitrarily set at 1.0. Results shown are the mean ± the range of values from both assays.

obtained from the adriamycin-treated mice, nuclear extracts from all mice in each group were pooled. DNA binding activity in both pooled samples was measured twice on different days. Surprisingly, both gel-shift assays showed an increase, not the expected reduction in NF-κB activation by LPS in macrophages from adriamycin-treated mice (Fig. 7). This result suggests that the impairment of cytokine formation we observed in macrophages from adriamycin-treated mice does not appear to occur at the level of NF-κB activation or nuclear translocation (Fig. 6).

Increased ROS formation and in macrophages from adriamycin-treated mice

To examine potential mechanisms underlying impaired macrophage recruitment and cytokine secretion, we first examined whether adriamycin treatment increases intracellular oxidative stress in peritoneal macrophages. To this end we loaded peritoneal macrophages from adriamycin- and saline-treated mice with the profluorescent redox-sensitive dye DCFH and measured the rate of fluorescent dye formation. The rate of DCFH oxidation was 2.1-fold higher in macrophages from adriamycin-treated compared to cells from saline-treated animals (Fig. 7), suggesting that adriamycin treatment increases ROS formation in tissue macrophages and this increase is sustained even 10 days after adriamycin treatment was stopped.

Increased protein-S-glutathionylation in macrophages from adriamycin-treated mice

Previously, we showed that in cultured human monocyte-derived macrophages adriamycin promotes glutathione disulfide formation and protein-*S*-glutathionylation [15]. We therefore determined whether low-dose adriamycin treatment also altered the glutathione redox state of macrophages in vivo. We observed no statistically significant change in the cellular content of either reduced glutathione (GSH) or glutathione disulfide (GSSG) in macrophages from saline- and adriamycin-treated mice and the GSH/GSSG ratio was identical in macrophages from both groups (not shown). However, protein-bound glutathione was increased by 35% in adriamycin-treated mice compared to saline-injected mice (Fig. 8),

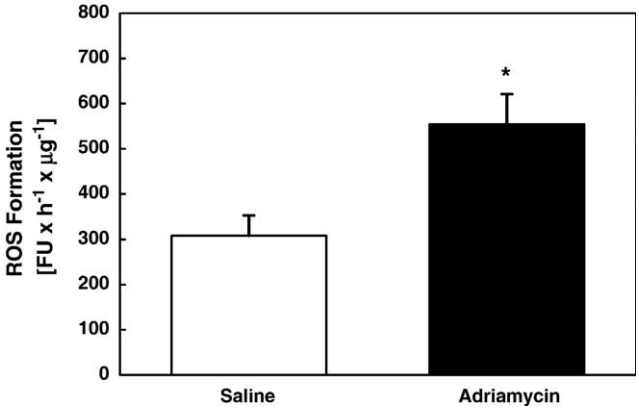

Fig. 7. Increased reactive oxygen species (ROS) formation in macrophages isolated from adriamycin-treated mice. Peritoneal macrophages were isolated from saline- (n = 13) and adriamycin-treated (n = 15) mice 10 days after the last injection and plated at 0.3 × 10^6 cells/ml for 3 h and nonadherent cells were removed by washing. Macrophages were loaded for 1 h at 37°C with 10 μg/ml DCFH and washed, and fluorescence was monitored for up to 9 h in a Fusion plate reader (Packard) as described under Materials and methods. ROS formation is expressed as rates of DCFH oxidation normalized to cell protein. Results are shown as mean ± SE. * $P < 0.05$.

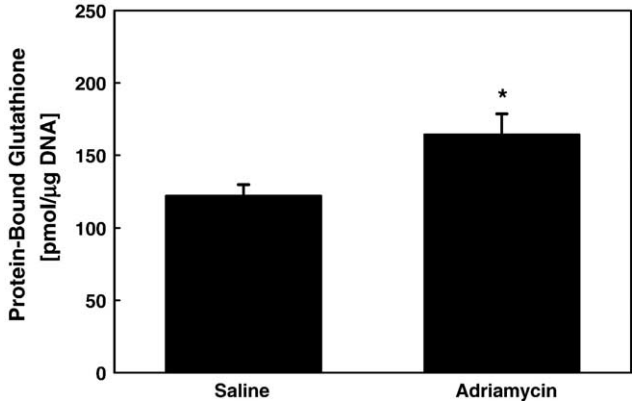

Fig. 8. Increased protein-*S*-glutathionylation in macrophages isolated from adriamycin-treated mice. Peritoneal macrophages were isolated from saline- ($n = 9$) and adriamycin-treated ($n = 9$) mice and plated at 1×10^6 cells/ml for 3 h and nonadherent cells were removed by washing. Macrophages were harvested by scraping and protein-bound glutathione (PSSG) was measured as described under Materials and methods. Results are shown as mean ± SE. * $P < 0.05$.

suggesting that even at low doses adriamycin treatment promotes sustained protein thiol oxidation in macrophages in vivo.

Discussion

Clinical and experimental evidence strongly suggests that adriamycin therapy impairs wound healing, but the mechanisms involved in this process remain unclear. Previously we showed that in cultured human macrophages adriamycin promotes GSSG formation and protein-*S*-glutathionylation and demonstrated that in macrophages thiol oxidation, rather than one-electron redox cycling and ROS generation, mediates adriamycin-induced cell damage [15]. The present study is the first to show that adriamycin promotes protein-*S*-glutathionylation in macrophages and impairs macrophage functions in vivo.

It has been well established that adriamycin therapy is associated with immunological deficits [3] and improving macrophage function with macrophage growth factors M-CSF and GM-CSF has been shown to improve wound healing in both animals and patients [31–33]. Hence, adriamycin-induced macrophage dysfunction would be a viable model to explain impaired tissue repair in chemotherapy patients. Macrophage dysfunction may also explain the 28% reduction in peritoneal cells in adriamycin-treated mice. Both enhanced rates of cell death and reduced blood monocyte levels could have accounted for this hypocellularity, but neither was observed in response to low doses of adriamycin. An alternative explanation for the reduced number of peritoneal macrophages would be decreased extravasation of blood monocytes into the peritoneum due to impaired chemotactic and migratory activity of blood monocytes in adriamycin-treated mice. The blunted macrophage recruitment in response to thioglycolate stimulation we observed in adriamycin-treated mice supports this hypothesis.

The hypothesis that adriamycin treatment promotes monocyte and macrophage dysfunction is further supported by our findings that macrophage cytokine and growth factor responses were significantly altered after adriamycin treatment. IL-1β and TNFα secretion- and VEGF release showed a similar trend-stimulated with LPS plus INFγ was reduced in macrophages from adriamycin-treated mice but TGFβ secretion was not affected. This suggests that the reduction in IL-1β, TNFα, and VEGF was not due to a general impairment of macromolecule synthesis. Instead, the mechanism underlying the impaired macrophage response in adriamycin-treated mice may involve increased intracellular oxidative stress as we found ROS formation and protein-*S*-glutathionylation to be significantly increased in macrophages from adriamycin-treated mice.

Adriamycin has redox-cycling properties and is a potent generator of intracellular oxidative stress and thiol oxidation [1,8,9,15]. In macrophages, LPS-induced IL-1β and TNFα formation is regulated by NF-κB, a redox-sensitive, pleiotropic transcription factor. Recently, VEGF expression in human macrophages was also shown to be NF-κB dependent [25]. Acute oxidative stress has been associated with the up-regulation of NF-κB [34]. However, more recent evidence suggests that long-term or chronic oxidative stress may inhibit NF-κB activation. For example, short-term incubation of macrophages with oxidized LDL (OxLDL), an inducer of oxidative stress in macrophages [35], activates NF-κB, but long-term treatment with OxLDL prevents LPS-induced NF-κB activation and blocks TNFα and IL-1β expression [36]. However, instead of the expected decrease we observed an increase in NF-κB activation in LPS-stimulated macrophages from adriamycin-treated mice. Our data would suggest that inhibition of cytokine and growth factor responses may occur downstream of NF-κB activation and translocation. Thiol oxidation in vitro was shown to inhibit DNA binding activity of NF-κB [37]. However, our EMSA results would also rule out impaired DNA binding as a mechanism to explain the reduced cytokine and growth factor responses. Thus, it appears that the impairment occurs at the transcriptional and/or translational level, although impaired protein secretion is also a conceivable mechanism.

Pharmacological studies indicate that adriamycin accumulates in multiple tissues and its release from these tissue compartments is only gradual. This is illustrated by a drug recovery in urine of only 50–60% after 4 to 5 days [3,38]. Our results suggest that adriamycin's redox-cycling properties combined with its prolonged retention in tissues are likely to promote a state of chronically elevated oxidative stress. Altered macrophage responsiveness was observed despite the 10-day recovery period, suggesting that macrophage dysfunction induced by chronic oxidative stress may not be a brief, transient down-regulation of selected responses but rather a long-term impairment of macrophage function. This hypothesis is supported by recently published results obtained in diabetic $Lepr^{db}$ mice. Peritoneal macrophages isolated from diabetic $Lepr^{db}$ mice show impaired IL-1β and TNFα release in response to LPS plus INFγ [39], very similar to the reduced response we observed in macrophages from adriamycin-treated mice. Like the adriamycin-treated mice in our study, wound healing is impaired in diabetic $Lepr^{db}$ mice when compared to

their nondiabetic littermates [40,41]. Diabetes is strongly associated with systemic oxidative stress [42] and macrophages play a crucial role in initiating and coordinating wound healing and tissue repair. Macrophage dysfunction induced by chronic oxidative stress may therefore contribute to impaired wound healing in both diabetic mice and mice treated with adriamycin.

In summary, our results show for the first time that adriamycin promotes sustained macrophage dysfunction in vivo. We propose that macrophage dysfunction may play an important role in impaired wound healing associated with adriamycin therapy in cancer patients.

Acknowledgments

This study was supported by NIH Grant RO1 HL-70963 (R.A.) and by Grant 85-001-16-IRG from the American Cancer Society (R.A.).

References

[1] Lothstein, L.; Israel, M.; Sweatman, T. W. Anthracycline drug targeting: cytoplasmic versus nuclear-a fork in the road. *Drug Resist. Updat.* **4:**169–177; 2001.

[2] Birtle, A. J. Anthracyclines and cardiotoxicity. *Clin. Oncol. (R. Coll. Radiol.)* **12:**146–152; 2000.

[3] Ehrke, M. J.; Mihich, E.; Berd, D.; Mastrangelo, M. J. Effects of anticancer drugs on the immune system in humans. *Semin. Oncol.* **16:**230–253; 1989.

[4] Bland, K. I.; Palin, W. E.; von Fraunhofer, J. A.; Morris, R. R.; Adcock, R. A.; Tobin, G. R. Experimental and clinical observations of the effects of cytotoxic chemotherapeutic drugs on wound healing. *Ann. Surg.* **199:**782–790; 1984.

[5] Devereux, D. F.; Thibault, L.; Boretos, J.; Brennan, M. F. The quantitative and qualitative impairment of wound healing by adriamycin. *Cancer* **43:**932–938; 1979.

[6] Harrison, L. E.; Port, J. L.; Hochwald, S.; Blumberg, D.; Burt, M. Perioperative growth hormone improves wound healing and immunologic function in rats receiving adriamycin. *J. Surg. Res.* **58:**646–650; 1995.

[7] Glass, C. K.; Witztum, J. L. Atherosclerosis: the road ahead. *Cell* **104:**503–516; 2001.

[8] Gewirtz, D. A. A critical evaluation of the mechanisms of action proposed for the antitumor effects of the anthracycline antibiotics adriamycin and daunorubicin. *Biochem. Pharmacol.* **57:**727–741; 1999.

[9] Horenstein, M. S.; Vander Heide, R. S.; L'Ecuyer, T. J. Molecular basis of anthracycline-induced cardiotoxicity and its prevention. *Mol. Genet. Metab.* **71:**436–444; 2000.

[10] Fry, M.; Green, D. E. Cardiolipin requirement for electron transfer in complex I and III of the mitochondrial respiratory chain. *J. Biol. Chem.* **256:**1874–1880; 1981.

[11] Fry, M.; Green, D. E. Cardiolipin requirement by cytochrome oxidase and the catalytic role of phospholipid. *Biochem. Biophys. Res. Commun.* **93:**1238–1246; 1980.

[12] Brunmark, A.; Cadenas, E. Redox and addition chemistry of quinoid compounds and its biological implications. *Free Radic. Biol. Med.* **7:**435–477; 1989.

[13] Garner, A. P.; Paine, M. J.; Rodriguez-Crespo, I.; Chinje, E. C.; Ortiz, D. M.; Stratford, I. J.; Tew, D. G.; Wolf, C. R. Nitric oxide synthases catalyze the activation of redox cycling and bioreductive anticancer agents. *Cancer Res.* **59:**1929–1934; 1999.

[14] Mimnaugh, E. G.; Trush, M. A.; Gram, T. E. Stimulation by adriamycin of rat heart and liver microsomal NADPH-dependent lipid peroxidation. *Biochem. Pharmacol.* **30:**2797–2804; 1981.

[15] Asmis, R.; Wang, Y.; Xu, l. ;M.; Kisgati, J. G.; Begley, J. J. A novel thiol oxidation-based mechanism for adriamycin-induced cell injury in human macrophages. *FASEB J.* **19:**1866–1868; 2005.

[16] Bertazzoli, C.; Bellini, O.; Magrini, U.; Tosana, M. G. Quantitative experimental evaluation of adriamycin cardiotoxicity in the mouse. *Cancer Treat. Rep.* **63:**1877–1883; 1979.

[17] Sun, X.; Zhou, Z.; Kang, Y. J. Attenuation of doxorubicin chronic toxicity in metallothionein-overexpressing transgenic mouse heart. *Cancer Res.* **61:**3382–3387; 2001.

[18] Mori, R.; Kondo, T.; Ohshima, T.; Ishida, Y.; Mukaida, N. Accelerated wound healing in tumor necrosis factor receptor p55-deficient mice with reduced leukocyte infiltration. *FASEB J.* **16:**963–974; 2002.

[19] Molloy, P. L. Electrophoretic mobility shift assays. *Methods Mol. Biol.* **130:**235–246; 2000.

[20] Dignam, J. D.; Lebovitz, R. M.; Roeder, R. G. Accurate transcription initiation by RNA polymerase II in a soluble extract from isolated mammalian nuclei. *Nucleic Acids Res.* **11:**1475–1489; 1983.

[21] Shamberger, R. C.; Devereux, D. F.; Brennan, M. F. The effect of chemotherapeutic agents on wound healing. *Int. Adv. Surg. Oncol.* **4:**15–58; 1981.

[22] Singal, P. K.; Iliskovic, N. Doxorubicin-induced cardiomyopathy. *N. Engl. J. Med.* **339:**900–905; 1998.

[23] Sun, X.; Zhou, Z.; Kang, Y. J. Attenuation of doxorubicin chronic toxicity in metallothionein-overexpressing transgenic mouse heart. *Cancer Res.* **61:**3382–3387; 2001.

[24] Lefrak, E. A.; Pitha, J.; Rosenheim, S.; Gottlieb, J. A. A clinicopathologic analysis of adriamycin cardiotoxicity. *Cancer* **32:**302–314; 1973.

[25] Kiriakidis, S.; Andreakos, E.; Monaco, C.; Foxwell, B.; Feldmann, M.; Paleolog, E. VEGF expression in human macrophages is NF-kappaB-dependent: studies using adenoviruses expressing the endogenous NF-kappaB inhibitor IkappaBalpha and a kinase-defective form of the IkappaB kinase 2. *J. Cell Sci.* **116:**665–674; 2003.

[26] Korn, S. H.; Wouters, E. F.; Vos, N.; Janssen-Heininger, Y. M. Cytokine-induced activation of nuclear factor-kappa B is inhibited by hydrogen peroxide through oxidative inactivation of IkappaB kinase. *J. Biol. Chem.* **276:**35693–35700; 2001.

[27] Reynaert, N.; Ckless, K.; van der Vliet, A.; Wouters, E.; Janssen-Helsinger, Y. Inactivation and glutathionylation of IKKβ by H_{2O2}. *Free Radic. Biol. Med.* **35:**S72; 2004.

[28] Chen, F. E.; Huang, D. B.; Chen, Y. Q.; Ghosh, G. Crystal structure of p50/p65 heterodimer of transcription factor NF-kappaB bound to DNA. *Nature* **391:**410–413; 1998.

[29] Nishi, T.; Shimizu, N.; Hiramoto, M.; Sato, I.; Yamaguchi, Y.; Hasegawa, M.; Aizawa, S.; Tanaka, H.; Kataoka, K.; Watanabe, H.; Handa, H. Spatial redox regulation of a critical cysteine residue of NF-kappa B in vivo. *J. Biol. Chem.* **277:**44548–44556; 2002.

[30] Pineda-Molina, E.; Klatt, P.; Vazquez, J.; Marina, A.; Garcia, d. L.; Perez-Sala, D.; Lamas, S. Glutathionylation of the p50 subunit of NF-kappaB: a mechanism for redox-induced inhibition of DNA binding. *Biochemistry* **40:**14134–14142; 2001.

[31] Wu, L.; Yu, Y. L.; Galiano, R. D.; Roth, S. I.; Mustoe, T. A. Macrophage colony-stimulating factor accelerates wound healing and upregulates TGF-beta1 mRNA levels through tissue macrophages. *J. Surg. Res.* **72:**162–169; 1997.

[32] Groves, R. W.; Schmidt-Lucke, J. A. Recombinant human GM-CSF in the treatment of poorly healing wounds. *Adv. Skin Wound Care* **13:**107–112; 2000.

[33] Fernberg, J. O.; Brosjo, O.; Friesland, S.; Masucci, G. GM-CSF at relatively high topic concentrations can significantly enhance the healing of surgically induced chronic wounds after radiotherapy. *Med. Oncol.* **18:**231–235; 2001.

[34] Schreck, R.; Albermann, K.; Baeuerle, P. A. Nuclear factor kappa B: an oxidative stress-responsive transcription factor of eukaryotic cells (a review). *Free Radic. Res. Commun.* **17:**221–237; 1992.

[35] Asmis, R.; Begley, J. G. Oxidized LDL promotes peroxide-mediated mitochondrial dysfunction and cell death in human macrophages: a caspase-3-independent pathway. *Circ. Res.* **92:** E20–E29; 2003.

[36] Brand, K.; Eisele, T.; Kreusel, U.; Page, M.; Page, S.; Haas, M.; Gerling, A.; Kaltschmidt, C.; Neumann, F. J.; Mackman, N.; Baeuerle, P. A.; Walli, A. K.; Neumeier, D. Dysregulation of monocytic nuclear factor-kappaB by

oxidized low-density lipoprotein. *Arterioscler. Thromb. Vasc. Biol.* **17:**1901–1909; 1997.

[37] Toledano, M. B.; Leonard, W. J. Modulation of transcription factor NF-kappa B binding activity by oxidation-reduction in vitro. *Proc. Natl. Acad. Sci. U. S. A.* **88:**4328–4332; 1991.

[38] Di Fronzo, G.; Lenaz, L.; Bonadonna, G. Distribution and excretion of adriamycin in man. *Biomedicine* **19:**169–171; 1973.

[39] Zykova, S. N.; Jenssen, T. G.; Berdal, M.; Olsen, R.; Myklebust, R.; Seljelid, R. Altered cytokine and nitric oxide secretion in vitro by macrophages from diabetic type II-like db/db mice. *Diabetes* **49:** 1451–1458; 2000.

[40] Tsuboi, R.; Rifkin, D. B. Recombinant basic fibroblast growth factor stimulates wound healing in healing-impaired db/db mice. *J. Exp. Med.* **172:**245–251; 1990.

[41] Greenhalgh, D. G.; Sprugel, K. H.; Murray, M. J.; Ross, R. PDGF and FGF stimulate wound healing in the genetically diabetic mouse. *Am. J. Pathol.* **136:**1235–1246; 1990.

[42] Keaney, J. F., Jr.; Larson, M. G.; Vasan, R. S.; Wilson, P. W.; Lipinska, I.; Corey, D.; Massaro, J. M.; Sutherland, P.; Vita, J. A.; Benjamin, E. J. Obesity and systemic oxidative stress: clinical correlates of oxidative stress in The Framingham Study. *Arterioscler. Thromb. Vasc. Biol.* **23:**434–439; 2003.